Monografías del Seminario Matemático García de Galdeano **33**, 121–128 (2006)

FORMULATION AND COMPUTATIONAL ASPECTS ON THE SIMULATION OF FRACTURE HEALING

M. J. Gómez-Benito, J. M. García-Aznar and M. Doblaré

Abstract. Fracture healing is a natural process that can reconstitute the fractured bone and recover its original function and form. In this work we extend to three dimensions a mechanobiological two dimension model of fracture healing based on mechanical stimulus. This model is able to model growth, differentiation and damage of the tissues that appear during the healing process. The continuity equation governs the evolution of the different cells and tissues.

Keywords: Computational mechanobiology, fracture healing, finite element.

AMS classification: 65L60.

§1. Introduction

When a bone fractures, it regenerates without scar, often restoring its initial geometry and stiffness, in contrast to other living tissues. This process of fracture healing is very complex. It implies migration, differentiation, proliferation and death of stem cells; and migration and death of fibroblasts, chondrocytes and osteoblasts which synthesize different types of tissues (granulation, fibrous, cartilage and bone tissue) [1]. The process of bone healing is affected by many different influences, such as growth factors, hormones and nutrients, the electrical and mechanical environments [2], etc. A good understanding of the specific influence of each of the factors that drive the healing process is important due to the social and economic impact of bone fractures, including surgery, long healing periods, infections, among many other aspects. In this work a mechanobiological model of fracture healing and its implementation in a finite element code is presented. This model is applied to simulate the bone healing process under bending loads.

§2. Material and methods

2.1. Model definition

Bone healing is a complex process in which coupling between cellular processes (differentiation, proliferation, migration) and callus growth exists. The main problem when simulating fracture healing is the coupling of both effects, since growth is associated to a change in the domain of study. In this work, the model of fracture healing previously developed by the same authors [3] was used. A brief description of this model is here presented while a more detailed

explanation can be found in the cited work. After fracture, macrophages migrate to the fracture site removing the death tissue and preparing the matrix to the migration of mesenchymal stem cells (MSCs). These MSCs and other cells populations are modelled in our case by their concentrations (c_i). MSCs come from three different origins periosteum, surrounding soft tissues and endosteum. In this work we have assumed that the main source of MSCs is the periosteum [4, 5]. MSCs can proliferate, migrate and differentiate. We assume that all these cellular processes are controlled by the mechanical stimulus, particullary by the second invariant of the deviatoric strain tensor ($\psi(\mathbf{x},t) = \sqrt{(\varepsilon_{ij} - \delta_{ij}\varepsilon_{kk}/3)(\varepsilon_{ij} - \delta_{ij}\varepsilon_{kk}/3)}$ with ε_{ij} the Cauchy strain tensor) [6, 7]. And thus, MSC proliferation is guided by this mechanical stimulus following:

$$\beta_s^{pr} = \frac{\alpha_{proliferation} \cdot \psi(\mathbf{x},t)}{\psi(\mathbf{x},t) + \psi_{proliferation}}, \tag{1}$$

where β_s^{pr} is stem cells proliferation rate, $\alpha_{proliferation}$, $\psi_{proliferation}$ are constants that define stem cell proliferation rate [3]. MSCs are assumed to proliferate until a saturation concentration (c_{smax}). When this concentration is achieved, the only way to further proliferate is increasing the size of the domain at a constant level of cell concentration (callus growth):

$$f^v_{proliferation} = \begin{cases} 0, & \text{if } (c_s < c_{smax}), \\ \beta_s^{pr} \dfrac{c_s}{c_{smax}}, & \text{if } (c_s = c_{smax}), \end{cases} \tag{2}$$

with $f^v_{proliferation}$ function that describes the callus growth through stem cell proliferation. Stem cells can also migrate. This migration is modelled as a random diffusion process which follows Fick's law. MSCs can also differentiate into chondrocytes (c_c), fibroblasts (c_f), osteoblasts (c_b) or they can die (c_d) (the death of MSCs is considered a specific differentiation pathway). This differentiation pathways are assumed to be determined by:

$$\begin{aligned}
&\text{if } (\psi_b < \psi < \psi_c), && \frac{Dc_c}{Dt} = \begin{cases} c_s, & \text{if } (t > t_m^c), \\ 0, & \text{otherwise}, \end{cases} \\
&\text{if } (\psi_c < \psi < \psi_f), && \frac{Dc_f}{Dt} = \begin{cases} c_s, & \text{if } (t > t_m^f), \\ 0, & \text{otherwise}, \end{cases} \\
&\text{if } (\psi_{lim} < \psi < \psi_b), && \frac{Dc_b}{Dt} = \begin{cases} D(\psi)\nabla^2 c_b, & \text{if } (t > t_m^b) \ \& \ (c_b < c_b^{min}), \\ c_s, & \text{if } (t > t_m^b) \ \& \ (c_b > c_b^{min}), \\ 0, & \text{otherwise}, \end{cases} \\
&\text{if } (\psi > \psi_d), && \frac{Dc_d}{Dt} = c_s,
\end{aligned} \tag{3}$$

where t_m^i is the time that stem cells need to differentiate into the different specialized cells (i), ψ_i is the mechanical stimulus level which indicates if MSCs can differentiate into cell i; c_b^{min} is the minimum concentration of bone cells that indicates when blood supply is completed at the ossification front and osteoblasts can differentiate directly from stem cells [3]. Later, cartilage cells hypertrophy and calcify increasing their volume and thus callus volume. This is another source of callus growth which is also assumed to be guided by the mechanical

stimulus following this expression:

$$g^{v}_{endochondral}(\psi,t) = -\frac{1}{c_c}\frac{Dc_c}{Dt} = \begin{cases} -\frac{1}{c_c}\left(\frac{\psi-\psi_{cal}}{\psi_b-\psi_{cal}}\cdot k_{hyper}\right), & \text{if } (c_c < c_{c_{min}}), \\ 0, & \text{otherwise}, \end{cases} \tag{4}$$

where $c_{c_{min}}$ is the equilibrium value of cartilage cell concentration; ψ_{cal} is the stimulus level below which cartilage begins to calcify; k_{hyper} is the parameter that controls the volume increase during cartilage calcification and $g^{v}_{endochondral}(\psi,t)$ function that describes the callus growth through chondrocytes hypertrophy. After hypertrophy, chondrocytes suffer programmed death (apoptosis) and allow osteoblasts to appear in the process of endochondral ossification; this is described by the equation:

$$\text{if } (\psi < \psi_b), \qquad \frac{Dc_b}{Dt} = \begin{cases} D(\psi)\nabla^2 c_b, & \text{if } (p_{mi} > p^{min}_{mi}) \;\&\; (c_b < c^{min}_{b}), \\ c_c, & \text{if } (p_{mi} > p^{min}_{mi}) \;\&\; (c_b > c^{min}_{b}), \\ 0, & \text{otherwise}, \end{cases} \tag{5}$$

where p_{mi} is the mineralization level, p^{min}_{mi} is the minimum mineralization level needed for endochondral ossification to take place. The bone formed in this process is a primary bone, that is, a very disorganized bone that is later replaced by a more organized one by means of an internal bone remodelling. In this analysis we have followed the remodelling model proposed by Beaupré et al. [8]. The extracellular matrix production is assumed to be proportional to the cell concentration [3]. All tissues are considered poroelastic and isotropic and composed by a fixed proportion of the following components: water, mineral, ground substance and collagens types I, II and III, being their mechanical properties determined by a mixture rule [9].

2.2. Numerical implementation

The numerical implementation of this model includes several coupled analysis combined with an automatic mesh generator. The whole process is controlled by an external program which manages all the needed information. The different steps of the process are:

1. *Introduction of bone and fracture geometry*. The simulations are performed in the central part (diaphysis) of a long bone which is assumed to be cylindrical [10, 9]. The parameters required are the radius of the diaphysis; width of the periosteum, endosteum, and bone marrow; size of the osteotomy gap; and the length of the diaphysis (Fig. 1).

2. *A cloud of nodes is generated.* Based on the geometry of the diaphysis a cloud of nodes is generated that reproduces the previous geometry. This cloud is denser near the fracture site and becomes looser far from the fracture to save computational cost (Fig. 1). Initial conditions are assigned to the main variables (cellular concentrations and extracellular matrix composition) associated to each node.

3. *Automatic mesh generation.* A tetrahedral mesh is automatically generated via an automatic mesh generator [11] based on the nodes introduced in (2).

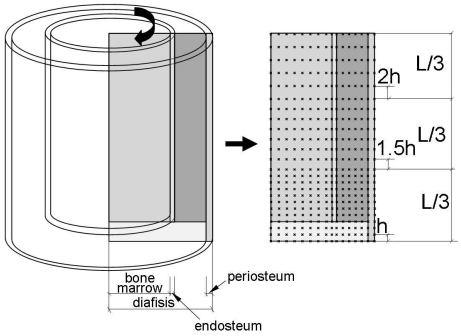

Figure 1: Definition of the geometry of the fracture and initial mesh generation.

4. *Finite element analyses.* Three different finite element analyses are performed in order to determine the evolution of the main variables and the geometry.

   (a) *Mechanical stimulus.* A poroelastic analysis is performed, in which the mechanical stimulus that will guide the different cell processes is determined.

   (b) *Migration of stem cells and advance of the ossification front.* Two independent diffusion analysis are performed. A diffusion analysis to simulate the migration of stem cells and another to determine the advance of the ossification front.

   (c) *Callus growth.* The growth of periosteal callus is assumed to be controlled by two processes: mesenchymal stem cell proliferation and chondrocyte hypertrophy. This growth is determined by means of a thermoelastic analysis, where the inverse of cell concentration, mesenchymal stem cell and chondrocyte, $(1/c_0^i)$, are identified with the expansion coefficients, while temperature is equivalent to the proliferation function ($f^v_{proliferation}$) or the growth of chondrocytes ($g^v_{endochondral}$). Thus, the new geometry and shape of the callus is defined by the node displacements obtained in this analysis.

5. *Update of cellular populations and extracellular matrix.* All main variables are updated by means of the model equations. These equations define the evolution of cell concentrations, extracellular matrix composition and the node position. Element mechanical properties are determined from the extracellular matrix composition at each point.

6. *Checking of the old mesh with the new geometry.* Based on the new location of the nodes, the elements are checked regarding: angle distortion and aspect ratio. If all the elements pass the check go to step (4) and start a new load increment; else continue to next step.

7. *Introduction of new nodes.* If any element does not fulfill the above conditions, a new node is generated at the center of the tetrahedron and its associated variables are interpolated from those corresponding to the vertices of that tetrahedron. For a boundary

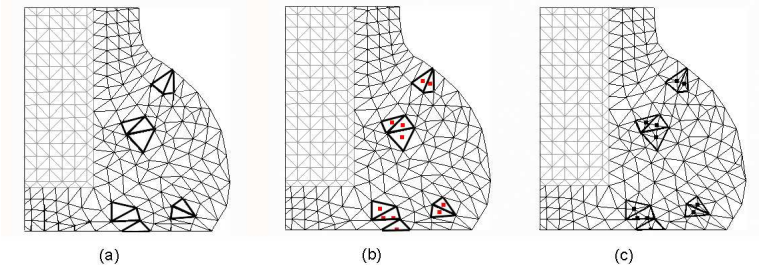

Figure 2: Introduction of nodes on the FE mesh (a) old mesh, (b) inclusion of new nodes, (c) remeshing (2D).

element with a big aspect ratio, a new node is added between the three existing boundary nodes (see Fig. 2). Then go to step (3) and start a new load increment.

§3. Results

The influence of bending loads is analyzed. A mid-diaphyseal fracture of a sheep tibia stabilized by a unilateral fixator is simulated. The unilateral fixator has been modelled with a 4mm radius circular section (Fig. 3.a). The fixator is attached only to one side of the bone by a screw of finite stiffness. Bone is loaded by an axial load of 500N [12]. In this case, a clear bending effect can be observed. The evolution of bone cells and of the callus geometry is not symmetrical in the screw plane as shown in figure 4 [13, 12].

Bone callus bridged sooner, about six weeks after fracture, in the lateral-frontal side (plane of the fixator, in the side nearer to the fixator) (Fig. 4.a). On the medial side the bridge occurs ten weeks after fracture and the callus results bigger. On the contrary, in the lateral plane (Fig. 4.b) the callus is symmetrical not only in geometry, but also in the evolution of the different cells.

This unsymmetrical fixation resulted in high bending movements in addition to the axial interfragmentary movement, causing a non symmetrical callus. A similar effect has been also observed in similar experimental tests [14].

§4. Discussion

Bone healing is a complex process in which the coupling between mechanical and geometrical problems is presented. The main difficulty in the implementation of this process is the "growth problem" in which a remeshing analysis is needed in each time increment to adapt the finite element mesh to the new geometry of the problem. In this work, a model previously used to study bone healing in 2D has been implemented in 3D to study the influence of compression-bending load on the bone healing process. In spite of the simplifications, this model has been qualitatively compared with experimental results, showing a remarkable similarity. Fractures healed with a unilateral fixator resulted in an unsymmetrical fracture callus in the screw plane in both geometry and tissue distribution due to the prevalence of bending

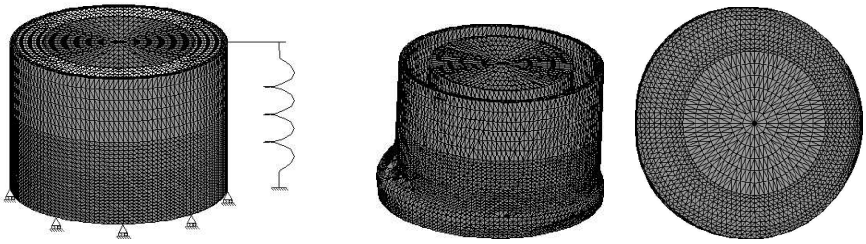

(a) (b)

Figure 3: (a) Initial finite element mesh and boundary conditions in the fracture stabilized by a unilateral fixator; and (b) final finite element mesh: frontal view and transverse plane.

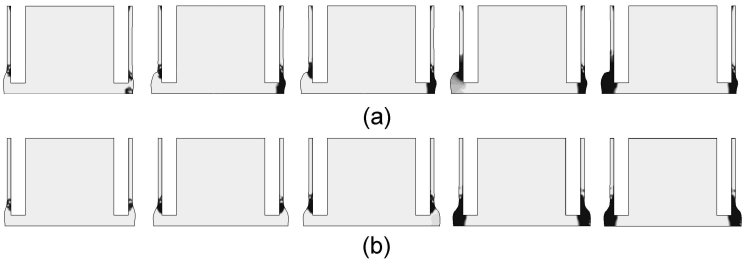

Figure 4: Osteoblast evolution (number of cells/mm^3) in (a) the frontal plane; (b) lateral plane for the fracture stabilized by a unilateral fixator.

loads. Hente et al. [14] also studied the effect in the bone healing process of compressive or distractive displacements. They developed a sheep experiment in which the gap was subjected to constant pure bending displacement, one side was supporting compressive loads, whereas the other supported tensile loads. They found important differences in the callus formed in the compressive and traction sides, both in callus size and tissue distribution. This similarity between computational and experimental results suggests that the observed effects can be explained largely by means of the mechano-biological model presented here. Nevertheless, we have to keep in mind that this simulation corresponds to an ideal situation, which is nearly impossible to be reproduced in a clinical study. In the simulation the callus was subjected to bending-compression load but in experimental studies on animals, it is almost impossible to isolate a single type of displacement or load. However, mathematical models implemented in computational simulations are valuable to investigate new othopaedic treatments. The use of these simulations can also help to reduce the number of experiments in animals.

Acknowledgements

Research partially supported by the Spanish Ministry of Science and Technology through the research project DPI2004-07410-C03-01. The authors would like to thank J. H. Kuiper (Keele University, U.K.) for his collaboration on the development of the bone fracture healing

model.

References

[1] EINHORN, T. A. Current concepts review: Enhancement of fracture-healing. *J. Bone Joint Surg. 77-A* (1995), 940–955.

[2] DIMITRIOU, R., TSIRIDIS, E., AND GIANNOUDIS, P. Current concepts of molecular aspects of bone healing. *Injury*, in press.

[3] GÓMEZ-BENITO, M. J., GARCÍA-AZNAR, J. M., KUIPER, J. H., AND DOBLARÉ, M. Influence of fracture gap size on the pattern of long bone healing: A computational study. *J. Theor. Biol. 235*, 1 (2005), 105–119.

[4] POSTACCHINI, F., GUMINA, S., PERUGIA, D., AND DE MARTINO, C. Early fracture callus in the diaphysis of human long bones. *Clin. Orthop. 310* (1995), 218–228.

[5] NUNAMAKER, D. M. Experimental models of fracture repair. *Clin. Orthop. 355S* (1998), 56–65.

[6] GARCÍA-AZNAR, J., KUIPER, J., DOBLARÉ, M., AND RICHARDSON, J. Computational simulation of fracture healing. In *Proceedings of the 13th Conference of European Society of Biomechanics*, R. Będzinski, C. Pezowicz, K., Ścigała, Eds. Wroclaw, Poland, 2002, pp. 394–395.

[7] ISAKSSON, H., WILSON, W., VAN DONKELAAR, C. C., HUISKES, R., AND ITO, K., Comparison of biophysical stimuli for mechano-regulation of tissue differentiation during fracture healing. *J. Biomech.*, DOI:10.1016/j.jbiomech.2005.01.037.

[8] BEAUPRÉ, G. S., ORR, T. E., AND CARTER, D. R. An approach for time-dependent bone modeling and remodeling-theoretical development. *J. Orthop. Res. 8* (1990), 551–651.

[9] LACROIX, D., AND PRENDERGAST, P. J. A mechano-regulation model for tissue differentiation during fracture healing: analysis of gap size and loading. *J. Biomech. 35* (2002), 1163–1171.

[10] CLAES, L. E., AND HEIGELE, C. A. Magnitudes of local stress and strain along bony surfaces predict the course and type of fracture healing. *J. Biomech. 32* (1999), 255–266.

[11] MÜCKE, E. *Shapes and Implementations in Three-Dimensional Geometry*. Ph.D. Thesis, University of Illinois at Urbana-Champaign, 1993.

[12] DUDA, G. N., ECKERT-HBNER, K., SOKIRANSKI, R., KREUTNER, A., MILLER, R., AND CLAES, L. Analysis of inter-fragmentary movement as a function of musculoskeletal loading conditions in sheep. *J. Biomech. 31*, 3 (1998), 201–210.

[13] YANG, L., NAYAGAM, S., AND SALEH, M. Stiffness characteristics and interfragmentary displacements with different hybrid external fixators, *Clin. Biomech. 18*, 2 (2003), 166–172.

[14] HENTE, R., FÜCHTMEIER, B., SCHLEGEL, U., ERNSTBERGERT, A., AND PERREN, S. M.. The influence of cyclic compression and distraction on the healing of experimental tibial fractures. *J. Orthop. Res. 22* (2004), 709–715.

M. J. Gómez-Benito, J. M. García-Aznar and M. Doblaré
Group of Structural Mechanics and Materials Modelling,
Aragón Institute of Engineering Research (I3A),
University of Zaragoza, María de Luna 3, 50015, Zaragoza, Spain
gomezmj@unizar.es , jmgaraz@unizar.es and mdoblare@unizar.es